Taylor & Francis
Taylor & Francis Group

ORIGINAL RESEARCH

∂ OPEN ACCESS   ⟳ Check for updates

Oncolytic influenza virus infection restores immunocompetence of lung tumor-associated alveolar macrophages

Dörthe Masemann[a,g], Katharina Köther[a,c], Meike Kuhlencord[b], Georg Varga[d], Johannes Roth[b,g], Brian Dennis Lichty[e], Ulf Rüdiger Rapp[f], Viktor Wixler[a,g], and Stephan Ludwig [iD][a,g]

[a]Institute of Virology (IMV), Westfaelische-Wilhelms University, Muenster, Germany; [b]Institute of Immunology, Westfaelische-Wilhelms University, Muenster, Germany; [c]Rentschler Biotechnologie GmbH, Laupheim, Germany; [d]Department of Pediatric, Rheumatology and Immunology, University Children's Hospital Muenster, Muenster, Germany; [e]Department of Pathology and Molecular Medicine, McMaster Immunology Research Centre, McMaster University, Hamilton, Ontario, Canada; [f]Max Planck Institute for Heart and Lung Research, Bad Nauheim, Germany; [g]Cluster of Excellence "Cells in Motion", University of Muenster, Muenster, Germany

ABSTRACT

Non-small-cell lung cancer (NSCLC) is the most frequent type of lung cancer and demonstrates high resistance to radiation and chemotherapy. These tumors evade immune system detection by promoting an immunosuppressive tumor microenvironment. Genetic analysis has revealed oncogenic activation of the Ras/Raf/MEK/ERK signaling pathway to be a hallmark of NSCLCs, which promotes influenza A virus (IAV) infection and replication in these cells. Thus, we aimed to unravel the oncolytic properties of IAV infection against NSCLCs in an immunocompetent model *in vivo*. Using *Raf-BxB* transgenic mice that spontaneously develop NSCLCs, we demonstrated that infection with low-pathogenic IAV leads to rapid and efficient oncolysis, eliminating 70% of the initial tumor mass. Interestingly, IAV infection of *Raf-BxB* mice caused a functional reversion of immunosuppressed tumor-associated lung macrophages into a M1-like pro-inflammatory active phenotype that additionally supported virus-induced oncolysis of cancer cells. Altogether, our data demonstrate for the first time in an immunocompetent *in vivo* model that oncolytic IAV infection is capable of restoring and redirecting immune cell functions within the tumor microenvironment of NSCLCs.

Introduction

Non-small-cell lung cancer (NSCLC) is the most frequent type of human lung cancer and displays low survival rates in patients. Although being insensitive to radiation and chemotherapy,[1,2] NSCLCs often establish an immunosuppressive tumor microenvironment that results in accumulation of suppressive immune cells, thus diminishing efficacy of immunotherapeutic approaches.[3,4] NSCLC originates from different lung epithelial cells, including central bronchi and terminal alveoli, but mainly from type II pneumocytes.[5,6] Genetic screening of human NSCLCs revealed frequent gain-of-function-mutations in epidermal growth factor receptor (*EGFR*) (20–40%)[7,8] or *K-Ras* (30%),[9,10] as well as amplified expression of the *c-Raf* kinase.[11-13] These alterations lead to hyperactivation of the Ras/Raf/MEK/ERK signaling cascade and stimulate neoplastic growth.[14] Despite significant understanding of the underlying causes of lung epithelial cell transformation, current therapies remain insufficient.

Within the last decades tumor cell-specific oncolytic viruses have developed into attractive cancer therapeutic approaches. Oncolytic viruses not only demonstrate constant lytic properties but are also highly immunogenic and redirect immune cells to the tumor site. In addition to several wildtype viruses, genetically-modified viruses have been tested in clinical trials.[15-17] In recent years, two important aspects of oncolytic viruses have been uncovered. First, tumors that are resistant to chemotherapy, radiotherapy or immunotherapy can still be susceptible to destruction by viruses, due to different underlying lytic mechanisms. Second, large scale tumor cells lysis releases numerous auto- and tumor-associated antigens (TAA), which in turn cause tissue inflammation and stimulate the immune system to enhance the anti-tumor effect initiated by viruses.[18] Interdependency of viral replication in tumor cells and immune responses against the tumor thus mainly determine efficacy of virotherapy.

Influenza A viruses (IAV) are negative-strand RNA viruses of the family of *Orthomyxoviruses*, primarily infecting type II lung epithelial cells in humans.[19] IAV-infected cells undergo apoptosis and cell death within a few hours.[20] Interestingly, activation of the Raf/MEK/ERK signaling cascade is essential for IAV replication and activation of this pathway strongly promotes viral replication.[21] Hence, NSCLC cells are not only

primary targets for IAV, but also exhibit an oncogenic activated Raf/MEK/ERK signaling cascade and are therefore likely to be highly sensitive to oncolytic IAVs. Indeed, a strong tropism of avian IAV for *raf*-transformed lung cancer cells has been previously demonstrated by us *in vivo* in a transgenic mouse model.[22] Although IAV infection has been shown previously by others to have oncolytic effects due to interferon-deficiency of *ras*-transformed cancer cells, these studies were exclusively performed *in vitro* or in *xenograft* models.[23-26] Moreover, the mutual interplay of tumor environment, immunosurveillance and oncolytic influenza A virus infection has not yet been studied in an immuocompetent model consistent with the human cancer phenotype. Since oncolytic virus-induced remodeling of the tumor environment and reactivation of the immune response against TAAs is pivotal for oncolytic virus efficacy and outcome in clinical studies, we provide novel data about oncolytic influenza A virus infection in a unique immunocompetent murine model of slowly growing, highly immune evasive NSCLCs. Tumor growth in the lungs of these mice is based on hyperactive ERK signaling in type II pneumocytes under a lung-specific promoter, thus closely resembling the human phenotype of NSCLCs. The principle of oncolytic influenza A virus efficacy is thus not only based on interferon-deficiency of NSCLC cells as but also the hyperactivation of the ERK signaling cascade that is known to promote influenza A virus replication primarily in NSCLC cells.

For the first time, we have demonstrated that IAV infection results in efficient lysis of NSCLC tumor cells *in vivo* and restores pro-inflammatory and anti-tumoral properties of formerly tumor-suppressed immune cells in the lung.

Results

IAV infection leads to efficient oncolysis of raf-transformed NSCLC in vivo

To study the oncolytic properties of a low pathogenic H1N1 human influenza A virus (PR8), tumor-bearing *Raf-BxB* transgenic mice were infected with a sublethal virus dose and NSCLC tumor tissue during IAV infection was determined along with virus spread. Paraffin-embedded lung sections were analyzed for human c-Raf and viral NP proteins using specific antibodies and the number of tumor foci per lung section as well as foci surface area in relation to the lung section was determined. To obtain a thorough representation of tumor tissue within the entire lung, three sections of each mouse lung that were at least 250 μm apart were analyzed.

Ongoing progression of IAV infection led to a remarkable decrease of both, number and size of lung tumors over time (Fig. 1). Tumor foci size diminished substantially during the first three days and continued to decline at a slower rate with the progression of infection. At day three post infection (p.i.), the tumor mass was reduced by up to 50% compared to tumors in non-infected control mice, and 70% of the original tumor mass was eradicated by day 12 post viral infection (Fig. 1A,D). Interestingly, the size of single foci and also the total numbers were already markedly reduced during the first three days of infection, and dropped significantly at later time points. At day 12 p.i. over 70% of the initial tumor foci were eliminated (Fig. 1A upper panel and C). Of note, a strong disintegration of distinct tumor foci structures was already apparent at day three p.i., as evidenced by immunostaining of lung sections analyzed at higher magnifications (Fig. 1B). As expected, reductions in
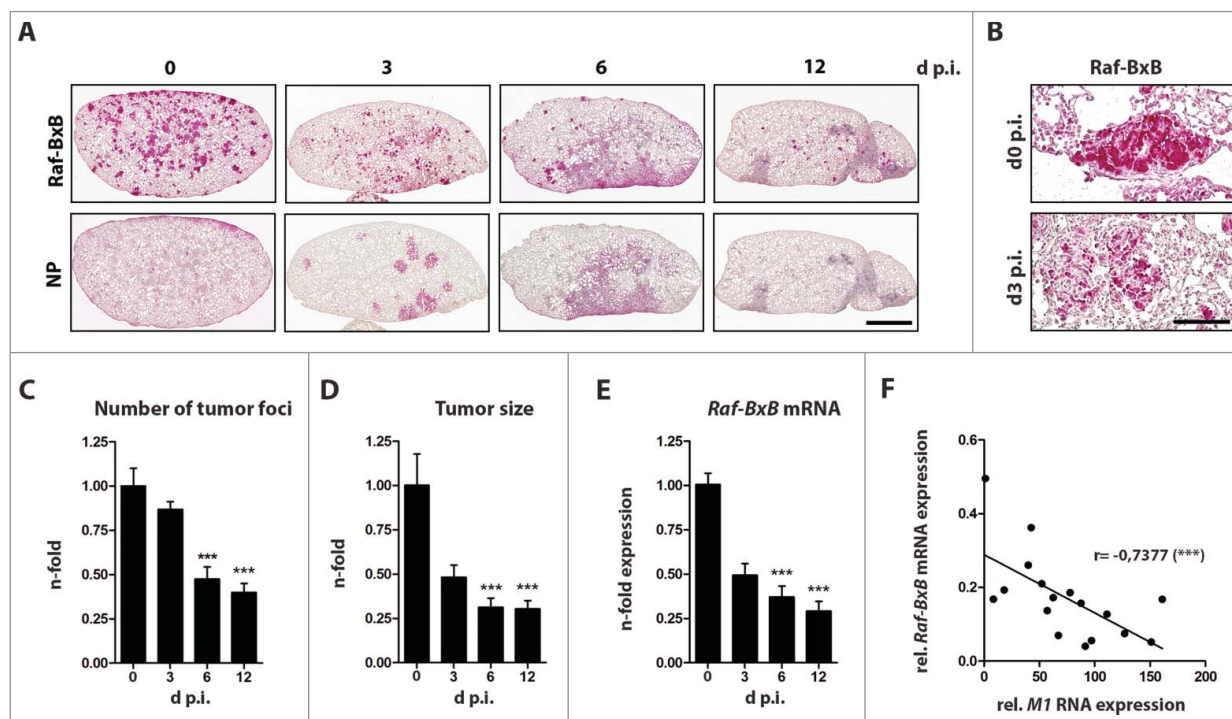
Figure 1. Influenza a virus infection mediates oncolysis of *raf*-transformed lung cancer tissue *in vivo*. *Raf-BxB* mice were infected with 500 particles of influenza A virus PR8 and at different days post infection lungs were analyzed for: (A and B), expression of human Raf-BxB and viral NP by immunohistochemistry; (C), number of tumor foci per lung; (D), relative size of tumor foci; (E), amount of human *Raf-BxB* mRNA transcripts by TaqMan qRT-PCR; (F), relative expression of oncogenic *Raf-BxB* and viral MI RNA. Mean values of uninfected control mice were arbitrarily taken as unity. Mean values $\pm$ SEM of two experiments with $\geq$5 animals per group in each experiment are presented. Always serial paraffin lung sections were used for stainings of Raf-BxB and NP. Bars = 2000 μm (A); 100 μm (B)

tumor tissue corresponded with reduced mRNA expression of the human *Raf-BxB* oncogenic transgene (Fig. 1E).

IAV infection reached a maximum at day 6 and declined thereafter, as evidenced by immunostaining of viral NP (Fig. 1A, bottom panel). At day 12 p.i. no viral NP protein was detectable in lungs of tumor-bearing mice. Strikingly, the increase in viral RNA expression correlated with the decreased expression of oncogenic human *Raf-BxB* (Fig. 1F), indicating a direct correlation of tumor lysis and viral replication efficiency. However to our surprise, we observed a decrease in tumor tissue not only in highly-infected lung areas, but also in non- or less-infected areas, suggesting additional involvement of host immune cells in conjunction with viral oncolytic activity in tumor destruction.

Viral replication is impaired in lungs of NSCLC-bearing mice

To evaluate the degree of viral infection and lung destruction in tumor-bearing mice, we compared the viral load in lungs of *Raf-BxB* and WT mice. We expected that infection of *Raf-BxB* mice would feature a more severe pathogenicity than in WT mice due to preferential replication of IAV in NSCLC cells with hyperactivated Ras/Raf/MEK/ERK signaling.[22] Surprisingly, IAV replication was reduced in tumor-bearing mice compared to WT mice when infected with the same viral dose. A tendency towards a reduced number of viral progeny in *Raf-BxB* compared to WT lungs was observed as early as day one p.i. and this trend became more pronounced over the course of infection, particularly at day three and six p.i. (Fig. 2A). The decreased replication rate of influenza viruses in Raf-BxB mice was further confirmed by comparative evaluation of viral *NP* mRNA amplification and viral NP protein distribution in lungs of *Raf-BxB* versus WT mice (Fig. 2B and C). Consistent with the lower viral load, lungs of tumor-bearing mice showed reduced mRNA expression levels of the *IL-6* and *TNFα* pro-inflammatory cytokines that usually accompany IAV infection and lung inflammation (Fig. 2D) as well as reduced lung tissue damage, indicated by a decreased release of soluble LDH protein into bronchoalveolar lavage fluid (BALF) (Fig. 2E). Finally, reduced IAV pathogenicity in *Raf-BxB* mice compared to WT mice was phenotypically confirmed by analyzing body weight
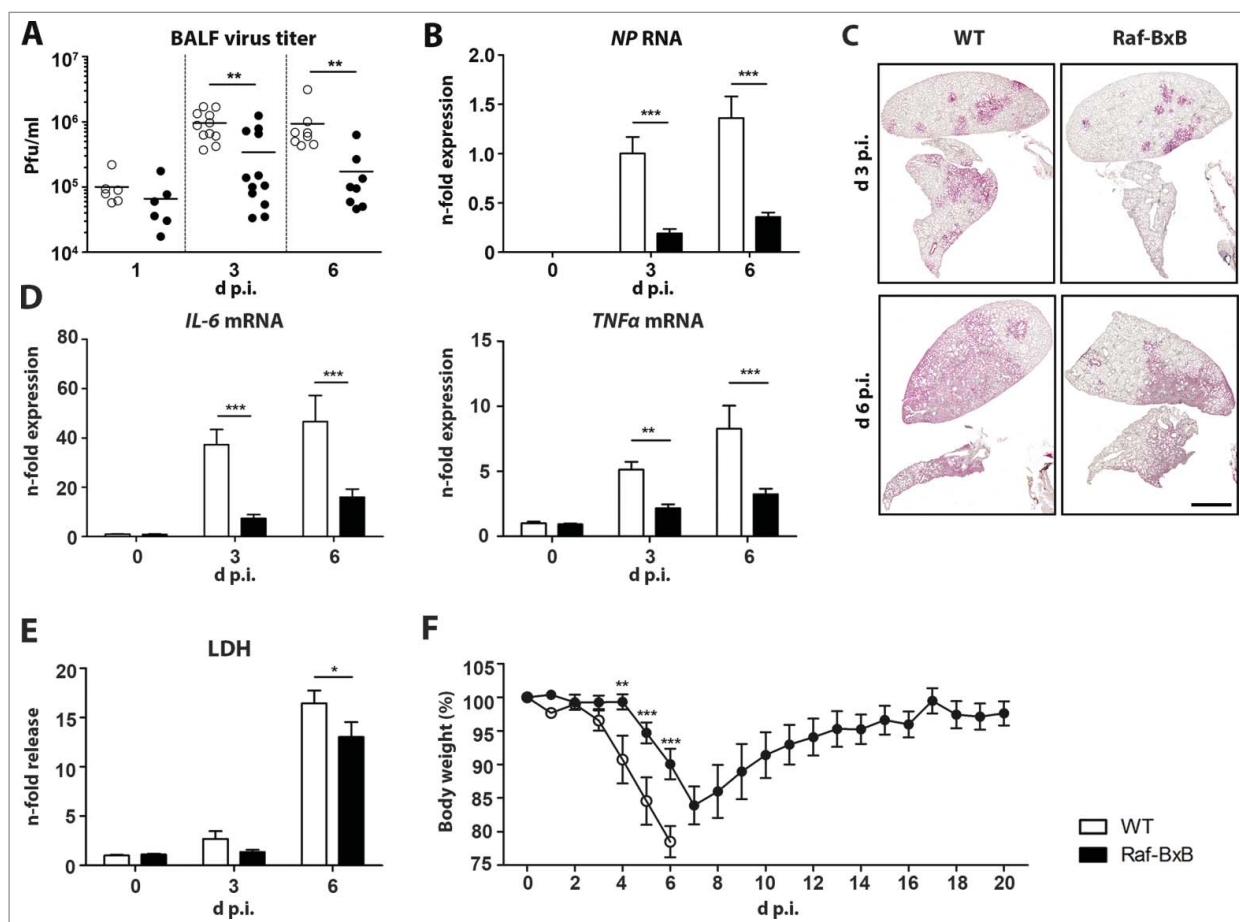
Figure 2. Comparative analysis of IAV replication in tumor-bearing and wildtype mice. C57Bl/6 WT and *Raf-BxB* mice were infected with 500 particles of IAV PR8 and at indicated days post infection, BALF and lung tissue were studied. (A) Virus titers presented as pfu/ml were determined in BAL samples by standard plaque assay. (B) RNA levels of viral *NP* were determined by qRT-PCR. The mean value of infected WT mice at day 3 p.i. was arbitrarily set to one. (C) Viral spread within the lungs of infected WT or *Raf-BxB* tumor-bearing mice was analyzed at day 3 and 6 post infection by immunohistochemistry staining of IAV NP protein. Bars = 2000 μm. (D) mRNA levels of pro-inflammatory cytokines *IL-6* and *TNFα* were determined by TaqMan qRT-PCR. Values of cytokines in uninfected WT mice were set as unity. (E) Relative LDH content in BALF of WT and *Raf-BxB* mice. The mean value of non-infected WT mice was set to one. (F) Bodyweight loss of infected WT and tumor-bearing *Raf-BxB* mice after IAV infection. Mean values ± SEM of two experiments with ≥5 animals per group in each experiment are presented.

changes and lethality of mice. Infection with a sublethal viral dose resulted in a significantly reduced body weight loss in *Raf-BxB* mice compared to WT animals. Moreover, all *Raf-BxB* mice recovered and survived the infection, while WT mice lost significantly more body weight to a level where they had to be euthanized in accordance with animal welfare regulations (Fig. 2F).

Accumulation of immunosuppressed tissue-resident alveolar macrophages in lungs of tumor-bearing mice

Many tumors, including NSCLCs, alter the local immune status, often by inducing accumulation of suppressive innate immune cells in the microenvironment[3,4] to support tumor progression. Hence, we asked whether the impaired replication of IAVs in NSCLC-bearing transgenic mice is due to alterations in the immune microenvironment in the lungs of *Raf-BxB* mice. To investigate the environmental role of tumor growth on immune cells in the direct tumor microenvironment in the lung, as well as in the bronchoalveolar space, immune cell subpopulations in both compartments were investigated by flow cytometry in comparison to WT mice.

Analysis of the total number of immune cells in BALFs revealed a drastically increased number of cells in tumor-bearing mice compared to WT (Fig. 3A). The vast majority of immune cells (>95 %) present in uninfected BALF of both

WT and tumor-bearing mice were classical tissue-resident alveolar macrophages ($CD11c^{hi}/F4/80^+/CD11b^-/Ly6C^-/Ly6G^-$) (Fig. 3B, Supplementary Figure 1A), however, the total number of alveolar macrophages was significantly increased in *Raf-BxB* mice (Fig. 3B, right). Furthermore, comparative analysis of immune cells in the BALF and lung tissue revealed predominant accumulation of alveolar macrophages not only in the BALF, but also in the lung compartment of *Raf-BxB* mice compared to WT mice (Supplementary Fig. 1B).

Deeper analysis of the predominant $CD11c^{hi}/F4/80^+$ alveolar macrophage population in the BALF revealed a reduced ratio of $MHCII^+$ cells in tumor-bearing mice compared to WT animals (Fig. 3C, Supplementary Figure 1C). Additionally, we detected a significantly increased number of macrophages that expressed $IL4R\alpha$ (Fig. 3D, Supplementary Fig. 1E), which is a marker for alternatively activated M2-like immunosuppressive macrophages. This indicates a strongly immunosuppressed phenotype of alveolar macrophages in the BALF of *Raf-BxB* mice. The proportion of cells expressing the pro-inflammatory enzyme iNOS was relatively low in lungs of *Raf-BxB* mice and did not significantly differ from that in WT mice (Fig. 3E), providing further evidence of immunologically inactive alveolar macrophages in BALF *Raf-BxB* mice. The very same immunosuppressed phenotype of alveolar macrophages was also found within the lung tissue of *Raf-BxB* mice (Supplementary Fig. 1D, 1F), as indicated by equally reduced levels of $MHCII^+$ and increased levels of $IL4R\alpha^+$ cells.
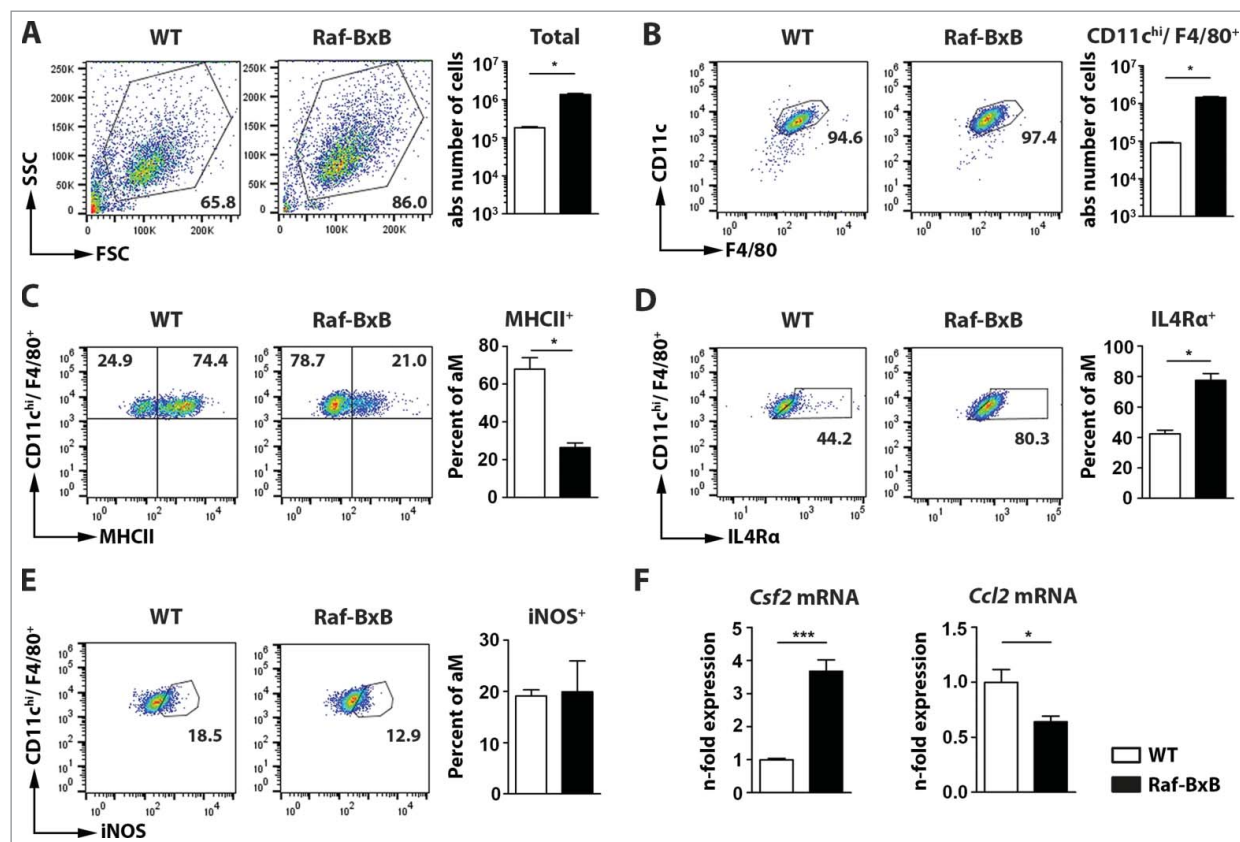
Figure 3. Accumulation of immunsuppressed alveolar macrophages in the lungs of tumor-bearing *Raf-BxB* mice. BAL fluids of non-infected WT and *Raf-BxB* mice were analyzed for presence of immune cells as well as for distinct populations of alveolar macrophages. (A), shows the total amount of cells in BALF per mouse. (B), represents the amount of alveolar macrophages with the phenotype of $CD11b^-/Ly6C^-/Ly6G^-/CD11c^{hi}/F4/80^+$. (C-E), Percentages of MHCII-, IL4Rα- or iNOS-positive alveolar macrophages (aM) are shown, respectively. Representative dot-blot images shown on the left underline the gating strategy used. (F), mRNA expression of *Csf2* and *Ccl2* in total lung lysates was analyzed via TaqMan qRT-PCR. The mean values of WT mice were arbitrarily taken as unity. Mean values ± SEM of two experiments with ≥5 animals per group in each experiment are shown.

These data demonstrate not only an increased accumulation of alveolar macrophages in both compartments, but also prove an equal level of immunosuppression of these cells by lung cancer growth independently of immune cell localization within the lungs of *Raf-BxB* mice.

To verify, if other macrophage subpopulations might also be differentially recruited to the lung of tumor-bearing *Raf-BxB* mice, levels of bone marrow-originating macrophages (CD45$^+$/F4/80$^+$/CD11b$^+$/Ly6C$^+$) (ΦM) in the BALF (Supplementary Fig. 1G) and lung compartments (Supplementary Fig. 1H) of *Raf-BxB* mice were investigated. Neither in BALF of WT nor of *Raf-BxB* mice, bone marrow-originating macrophages were detected (Supplementary Fig. 1G). Additionally, only minor percentages of CD45$^+$/F4/80$^+$/CD11b$^+$/Ly6C$^+$ macrophages (approx. 2% of all CD45$^+$ immune cells) could be found in the lungs of both, WT and *Raf-BxB* mice (Supplementary Figure 1H). Thus, we excluded a potential role of bone marrow-originating tumor-associated macrophages in the progression and immune evasion of NSCLCs in the lungs of *Raf-BxB* mice. Hence, our data demonstrate that the population of immunosuppressive alveolar macrophages analyzed in the BALF of *Raf-BxB* mice represents the major macrophages population affected by lung tumor growth in this mouse model.

We next examined whether the enhanced recruitment of macrophages to the lungs of *Raf-BxB* mice is consistent with increased expression of certain chemoattractants that are known to be responsible for macrophage recruitment and proliferation, namely *Csf2* (GM-CSF) and *Ccl2* (CCL2) (Fig. 3F). While the amount of total *Csf2* transcripts was highly increased in tumor-bearing mice compared to WT animals, the expression of *Ccl2* mRNA was significantly reduced (Fig. 3F). The enhanced levels of alveolar macrophages in the lungs of tumor-bearing mice is therefore most likely based on the increased expression of *Csf2* that is produced by tumor cells and on *in situ* proliferation of tissue-resident alveolar macrophages, because only cells with classical alveolar macrophage surface markers (SigF$^+$/CD11c^{hi}) but not with bone marrow monocyte markers (CD11b$^-$/Ly6C$^-$) were detected. These data are in agreement with earlier findings that certain non-small cell lung cancers of human patients secrete increased levels of GM-CSF.[27]

Soluble factors in the BALF of tumor-bearing mice lead to suppression of alveolar macrophages in the tumor microenvironment

Our results indicate a strong immunosuppression of alveolar macrophages in tumor-bearing mice. To investigate whether the NSCLC tumors of *Raf-BxB* mice indeed would promote an immunosuppressive environment, we cultured bone marrow-derived macrophages (CD11b$^+$/F4/80$^+$) in the presence of BALF from uninfected WT or *Raf-BxB* animals. Macrophages were isolated from WT mice to exclude a putatively immunosuppressed phenotype. BALF samples were sterile filtered before use, to avoid contamination by immune cells. Compared with BALF from WT mice, incubation of macrophages with BALF from *Raf-BxB* mice significantly reduced the percentage of macrophages expressing the activation marker MHCII (Fig. 4A) and simultaneously enhanced the amount of IL4Rα-positive cells (Fig. 4B). In comparison, the number of cells

expressing iNOS was not altered, but remained as low as in macrophages cultivated in the BALF of WT mice or medium alone (Fig. 4C).

When co-cultured with human cancer cells (HeLa), the cytotoxic activity of pre-activated bone marrow-derived macrophages (induced by o/n stimulation with LPS) was significantly diminished in the presence of BALF derived from *Raf-BxB* mice compared to WT mice (Fig. 4D) suggesting a functional inhibition of antitumoral cytotoxic activity of macrophages in the tumor microenvironment of *Raf-BxB* mice by soluble factors. These data indicate that one or more soluble factors in the BALF of NSCLC-bearing mice induce polarization of macrophages towards a M2-like anti-inflammatory phenotype resulting in a functional impairment of cytotoxic activity of these macrophages in the lungs of tumor-bearing mice.

IAV infection induces a pro-inflammatory immune response via alveolar macrophages in tumor-bearing mice

Our experiments showed that infection of *Raf-BxB* mice with IAV resulted in a fast and efficient lysis of NSCLC tumors, although viral infection of *Raf-BxB* mice was significantly milder than in WT mice. Additionally, we demonstrated that non-infected tumor-bearing *Raf-BxB* mice contain increased amounts of immunologically impaired tumor-associated macrophages in their lungs. These lung-resident macrophages, however, are known to be the first line of defense against viral infections. To explore whether the increased number of alveolar macrophages in *Raf-BxB* lungs was beneficial for anti-IAV immune response and possibly for IAV-mediated NSCLC tumor cell lysis, we compared the development of innate and adaptive immune responses in *Raf-BxB* and WT mice after infection with the same viral dose.

As expected, the number of immune cells in the bronchoalveolar space of WT mice increased significantly after IAV infection (Fig. 5A), *Raf-BxB* mice did not show a similar effect. The total number of immune cells was already high in non-infected mice and increased only slightly after IAV application. As expected, the number of alveolar macrophages exhibiting the CD11c^{hi}/F4/80$^+$/CD11b$^-$/Ly6C$^-$/Ly6G$^-$ phenotype decreased with infection in both WT and tumor-bearing mice and their kinetic profiles were similar.[28] However, *Raf-BxB* mice displayed at least a 10-fold excess in the absolute number of these cells in the bronchoalveolar space (Fig. 5B). The percentage of activated macrophages, represented by MHCII$^+$ (Fig. 5C) or iNOS$^+$ (Fig. 5D) cells increased after infection in both mouse types, but in contrast to the CD11c^{hi}/F4/80$^+$/CD11b$^-$/Ly6C$^-$/Ly6G$^-$ macrophage population, their numbers were consistently higher in WT mice. Nevertheless, after IAV infection the percentage of MHCII+ macrophages grew faster in tumor-bearing mice than in WT mice and almost reached equivalent levels at day six p.i. (Fig. 5C). The ratio of macrophages expressing the anti-inflammatory IL4Rα, to the contrary, being significantly larger in non-infected tumor-bearing mice, was equalized between WT and *Raf-BxB* mice at day six p.i. (Fig. 5E). Thus, the flow cytometry analysis indicates a phenotypic reversion of alveolar macrophages from an inactive CD11c^{hi}/F4/80$^+$/CD11b$^-$/Ly6C$^-$/Ly6G$^-$/MHCII$^-$/IL4Ra$^+$/iNOS$^-$ to an immunologically active CD11c^{hi}/ F4/80$^+$/CD11b$^-$/Ly6C$^-$/Ly6G$^-$/MHCII$^+$/IL4Ra$^+$/iNOS$^+$ status in *Raf-*
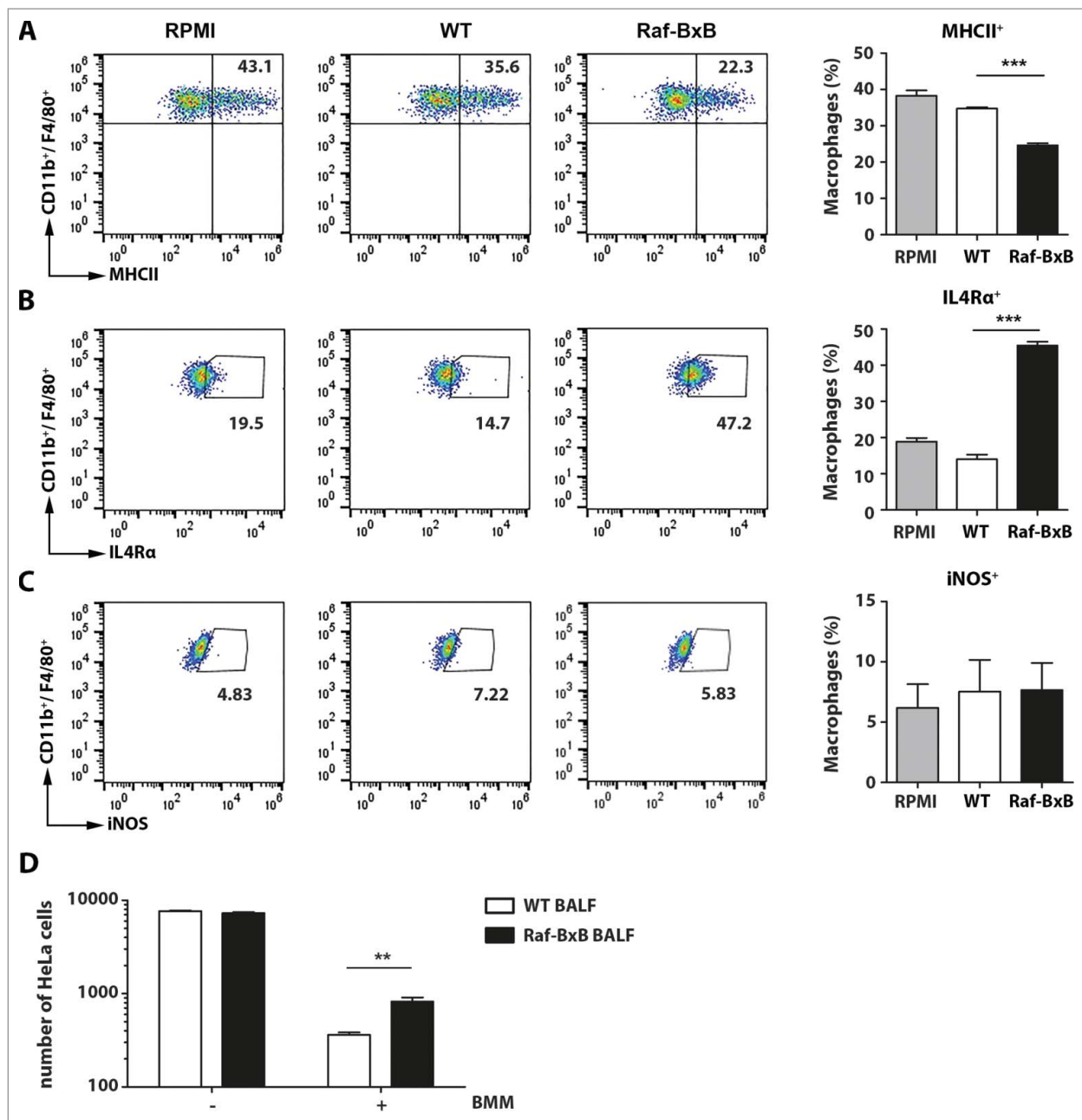
Figure 4. Incubation of bone marrow-derived macrophages with BALF from WT or tumor-bearing *Raf-BxB* mice. Bone marrow-cells from WT mice were isolated and differentiated to bone marrow-derived macrophages (BMM) (CD11b$^+$/ F4/80$^+$) by incubation with M-CSF for 5 days. (A, B, C) Then, the cells were re-cultured for 48h in the presence of BALF from uninfected WT or *Raf-BxB* mice or RPMI medium as control and analyzed for surface expression of MHCII (A) or IL4Rα (B) or intracellular expression of iNOS (C) by flow cytometry. Representative dot-blot images underlining the gating strategy are exemplarily shown. (D) BMM were pre-activated over night with 1 μg/ml LPS and afterwards co-cultured with mitomycin-treated HeLa cells in presence of BALF derived from WT or *Raf-BxB* mice (E/T = 20/1). 48h post co-culture, the absolute number of remaining HeLa cells was determined via flow cytometry by usage of cell counting beads. Mean values ±SEM are shown. BALF was isolated and pooled from at least 3 different mice . Bone marrow cells were pooled from 3 animals.

BxB mice after IAV infection (detailed gating strategies are shown in Supplementary Figure S2).

Interestingly, the mRNA expression of *Csf2* (GM-CSF) in the lungs of WT mice was low in uninfected animals, but significantly increased until day 6 p.i., as expected during acute respiratory infection (Fig. 5F). However, the expression of *Csf2* in the lungs of tumor-bearing mice was already significantly higher in non-infected NSCLC-bearing mice and decreased drastically after IAV infection, reflecting the observed reduction in tumor tissue. In comparison to the expression levels of *Csf2*, the major macrophage chemoattractant *Ccl2* (CCL2) (Fig. 5G)

showed a similar expression kinetic in *Raf-BxB* as in WT mice. The less pronounced levels in *Raf-BxB* mice were likely due to reduced viral replication in these animals.

IAV infection of Raf-BxB mice promotes repolarization from a suppressive to an activated pro-inflammatory phenotype of alveolar macrophages

During IAV infection of *Raf-BxB* mice, a drastic shift to immunologically activated alveolar macrophages was detected in
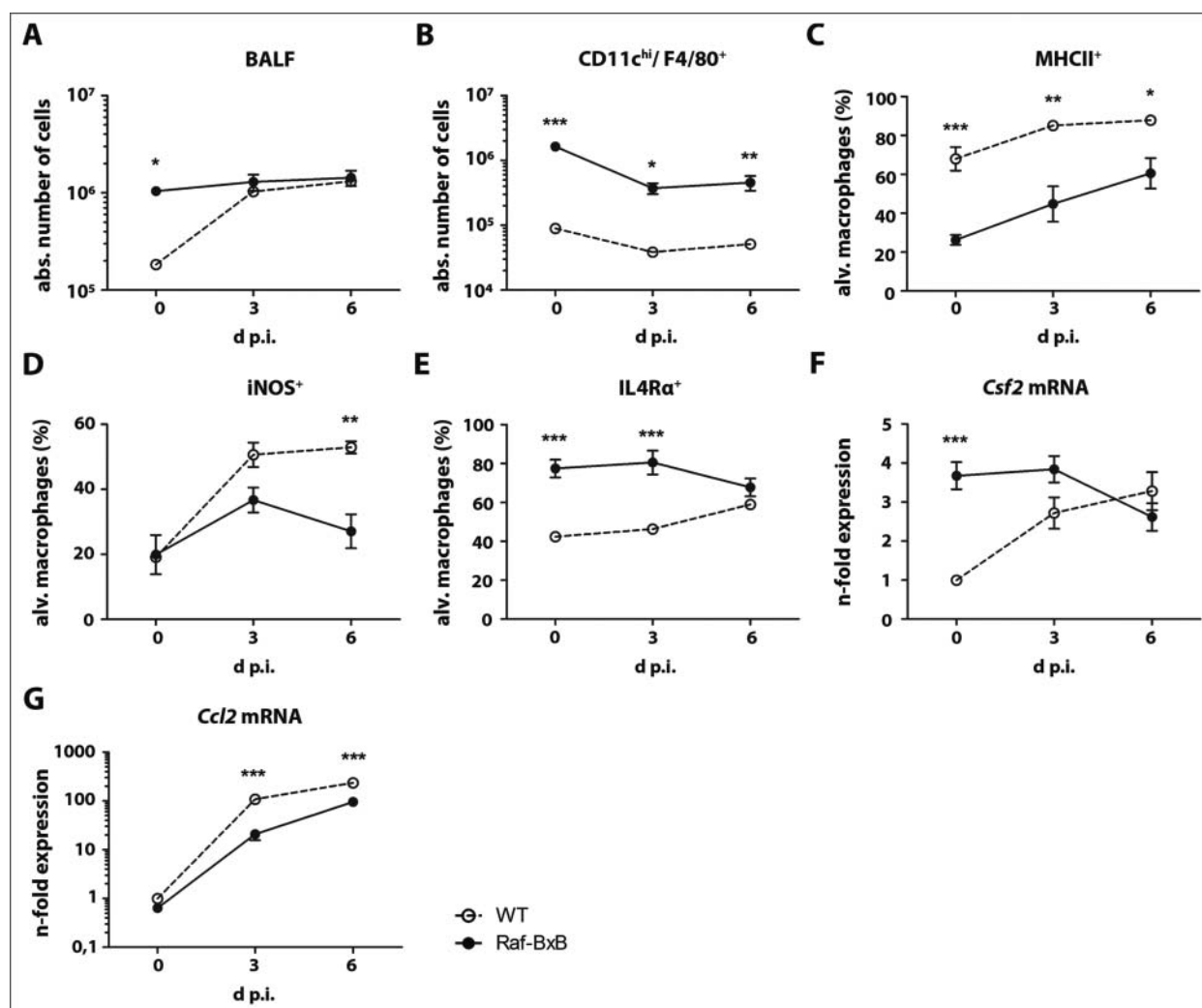
Figure 5. Anti-IAV immune responses in the lungs of WT and tumor-bearing *Raf-BxB* mice. C57Bl/6 WT and *Raf-BxB* mice were infected with 500 particles of IAV PR8 and at indicated times, the BALF were analyzed for presence of immune cells *per se* as well as for distinct populations of lymphocytes and alveolar macrophages. The absolute number of total immune cells (A) and alveolar macrophages (CD11b⁻/Ly6C⁻/Ly6G⁻/CD11cʰⁱ/F4/80⁺) per mouse are shown. Percentages of MHCII⁺(C), iNOS⁺ (D) and IL4Rα⁺ (E) alveolar macrophages are depicted. Representative dot-blot images underlining the gating strategy are shown in Figure S1. (F, G) mRNA expression levels of *Csf2* and *Ccl2* in total lung lysates were analyzed by TaqMan qRT-PCR. mRNA expression levels in uninfected WT mice were arbitrarily taken as unity. Mean values ± SEM of two experiments with ≥5 animals per group in each experiment are shown.

the lungs without any increase in their total amount. We considered two potential mechanisms: i) a switch in activation of formerly suppressed tissue resident macrophages or ii) an extensive recruitment of immunologically competent macrophages from other immune organs. To address this question, a fluorescent CMTMR dye was applied to lungs of *Raf-BxB* mice 24h before infection to discriminate between macrophages resident in the lungs before infection or macrophages recruited to the lungs subsequent to infection. Thus, alveolar macrophages were analyzed three days after IAV infection for their pro-inflammatory properties, comparing *Raf-BxB* with uninfected mice.

Four days after dye application, the vast majority of immune cells in the bronchoalveolar space of uninfected tumor-bearing mice were CMTMR positive (>97%), indicating efficient staining of lung resident immune cells (gating strategies are detailed in Supplementary Figure S3). As expected, the majority of these cells were alveolar macrophages (aM) exposing CD11cʰⁱ/F4/80⁺

surface markers (Fig. 6A) and exhibiting an immunologically inactive phenotype (MHCII⁻/IL4Rα⁺/iNOS⁻) (Fig. 6A, left panels). Three days after IAV infection, the majority of cells in the alveolar space were still positive for CMTMR dye (Supplementary Figure S3) and expressed typical markers for alveolar macrophages (CD11cʰⁱ/F4/80⁺/CD11b⁻/GR1⁻) but showed an enhanced portion of MHCII⁺ and iNOS⁺ cells (Fig. 6A, right panels). These data demonstrate that lung-resident and formerly immunosuppressed macrophages account for the activated macrophage population. This is remarkable, as it indicates that IAV infection triggers the formerly tumor-suppressed alveolar macrophages to switch to immunologically competent pro-inflammatory cells. The relative amount of cells expressing the alternative activation receptor IL4Rα, however, was hardly affected by IAV infection at day three post infection (Fig. 6A, lower panel).

The repolarization of tumor-associated alveolar macrophages was not only evident on a phenotypic, but also on a functional level. While the phagocytic activity of CD11cʰⁱ/
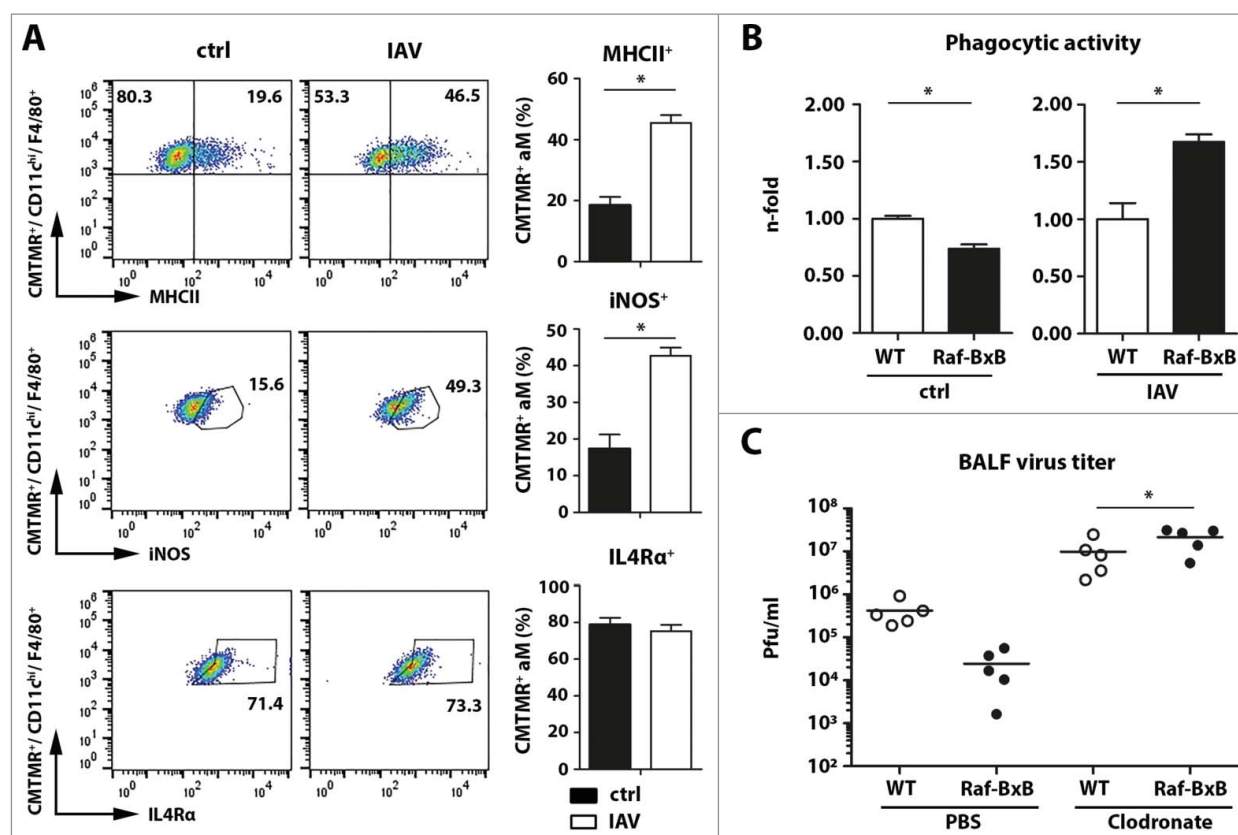
Figure 6. IAV infection of tumor-bearing mice activates immunosuppressed resident alveolar macrophages. (A), *Raf-BxB* mice were inoculated intranasally with 50 μl of 8 mM fluorescent CMTMR dye and 24h later, mice were either mock- (ctrl) or IAV infected (500 particles/ mouse). Three days post infection BALF was collected and immune cells were analyzed by flow cytometry. Monocytes present in the BALF were pre-gated on CMTMR$^+$ cells (representative dot plots indicating the gating strategie shown in Supplementary Figure S3). CMTMR$^+$/CD11c^{hi}/F4/80$^+$ alveolar macrophages (aM) were analyzed for expression of MHCII, iNOS or IL4Rα before (ctrl) and three days post infection (IAV). Representative dot-blot images underlining the gating strategy are exemplarily shown. (B), Immune cells from the BALF of mock- or IAV-infected mice were isolated 3 d.p.i. and incubated with fluorescent *E.coli* bioparticles. Phagocytic activity of CD11c^{hi}/F4/80$^+$ alveolar macrophages was investigated via flow cytometry and represented by relative amounts of CD11c^{hi}/F4/80$^+$ cells positive for uptake of fluorescent bioparticles. The mean value of WT mice were arbitrarily takes as unity. (C), WT and Raf-BxB mice were inoculated intranasally with PBS- or Clodronate-containing liposomes and 24h later, mice were infected with IAV. Three d.p.i., BALF was analyzed for virus titers (pfu/ml) via standard plaque assay. Mean values ±SEM of 5 animals per group are shown.

F4/80$^+$ macrophages was significantly impaired in the lungs of *Raf-BxB* mice before infection (Fig. 6B, left panel), it was even significantly increased 3 days post influenza virus infection and was almost two-times higher than in WT mice (Fig. 6B, right panel). In summary, these findings revealed that influenza virus infection induces a switch in activation of formerly immunosuppressed alveolar macrophages in the lungs of NSCLC-bearing mice to pro-inflammatory active macrophages.

As shown in Fig. 2, virus replication and pathogenicity was significantly reduced in *Raf-BxB* mice. To analyze whether alveolar macrophage accumulation and repolarization in the lungs of tumor-bearing *Raf-BxB* mice may be responsible for this unexpected phenotype, alveolar macrophages were depleted by intranasal administration of clodronate-filled liposomes 24h before infection. Monocytes engulfing clodronate-containing liposomes die by apoptosis due to irreversible damage, while PBS-filled liposomes serve as a control. As expected, administration of PBS-filled control liposomes did not alter viral replication three days p.i. and resulted in ten-fold decreased viral replication on the lungs of *Raf-BxB* mice compared to WT mice (Fig. 6C). In contrast, depletion of alveolar macrophages resulted in an overall increase of viral titers, which is consistent with previous data.[29] Interestingly, viral titers in the lungs of

Raf-BxB mice were twice as high as in WT mice, supporting the protective role of accumulation and reactivation of tumor-associated alveolar macrophages in the lungs of *Raf-BxB* mice leading to a suppression of influenza virus propagation.

Discussion

The primary goal of any cancer therapy is to selectively destroy tumor cells, limiting collateral damage of the surrounding tissue to a minimum. Although viruses are considered to be invasive pathogens and are commonly associated with harmful or severe diseases, their prospects have been considered for many years as therapeutic agents against cancer. The potential of influenza viruses as anti-NSCLC therapeutic agents is based on three facts. First, genetic analysis of human NSCLCs has shown that their aggressive neoplastic growth is almost exclusively based on oncogenic activation of the Ras/Raf/MEK/ERK signaling cascade.[7,8,10,14] Second, replication of influenza viruses *per se* is host cell destructive[30-32] and strongly depends on activation of the cellular Ras/Raf/MEK/ERK pathway. Third, type II alveolar pneumocytes are the natural primary targets for both, neoplastic transformation to NSCLCs and infection by IAV infection.[5,6,15,18]

The general oncolytic potential of Influenza A viruses was previously described *in vitro* and *ex vivo*, mainly focusing on interferon-deficiency of several human cancer cell lines.[23-26] A few *in vivo* studies of influenza A virus oncolytic potential have been performed solely in highly immunoincompetent murine *xenograft* models.[25,33] Thus, interdependency of tumor development, immune cell polarization, influenza A virus replication and tumor cell oncolysis has remained largely unknown. Knowledge regarding immune remodeling in the tumor environment, as well as virus-induced immune responses, is pivotal for oncolytic virus efficacy and outcome in clinical studies in patients.

Thus, we aimed to analyze the oncolytic properties of a low pathogenic human IAV in an immunocompetent *in vivo* model of NSCLC to unravel the general feasibility of low pathogenic human oncolytic influenza A virus infection in the context of slowly growing immune evasive NSCLCs. *Raf-BxB* mice are regarded as an ideal animal model, closely resembling the phenotype found in patients.[34] Strikingly, IAV infection appears to be highly effective in NSCLC cell destruction: three days after infection tumor foci were efficiently disintegrated and reduced in numbers. This effect even advanced with ongoing viral progression, reaching a 70% decrease of tumor mass at day 12 post infection. Moreover, the efficiency of tumor destruction was proven to be directly dependent on the viral replication rate.

Interestingly, reduction of NSCLC tumor-tissue was evident not only in highly infected lung areas, but also as a global effect in the whole lung. In addition, infection of tumor-bearing mice resulted in impaired viral replication and, infected *Raf-BxB* mice displayed increased survival in comparison to WT mice. We expected the opposite effect, given the pro-viral properties of the hyperactivated ERK signaling cascade in NSCLC cells. These findings thus imply a potential engagement of the immune system, which would be consistent with the action of several other oncolytic viruses that rapidly activate the immune system to facilitate tumor cell lysis.[35]

The high percentage of immune cells in tumor microenvironments, including tumor-associated macrophages, is a well-studied characteristic for many types of tumors. These immune cells are commonly immunosuppressed by tumor cells and support the growth of neoplastic cells rather than destroy them.[3,4] On the other hand, cells of the immediate innate immune response present in the lung strongly affect the outcome of respiratory infections. In the current study, comparison of the immune cell status in lungs of tumor-bearing and WT mice revealed a massive accumulation of tissue-resident alveolar macrophages in the lungs of *Raf-BxB* mice. As well as an increase in total number, alveolar macrophages were also strongly immunosuppressed, as indicated by increased levels of CD11c^{hi}/F4/80$^+$/MHCII$^-$/IL4Ra$^+$/iNOS$^-$ cells. Our findings imply that one or more soluble factor(s), most likely released by tumor cells, are responsible for immunosuppression of alveolar macrophages resulting in a tumor-promotive phenotype. Their increased occurrence in the lung is, in turn, induced by over-expression of *Csf2*, increased amounts of which were found in tumor-bearing *Raf-BxB* mice. Factors such as M-CSF (*Csf1*) or GM-CSF (*Csf2*) have been shown not only to promote myelopoiesis and proliferation of monocytes, but also to enhance recruitment and proliferation of TAMs in several tumor models.[36,37] Concomitantly, increased expression of *Csf2* by different kinds of human and murine cancers promoted tumor progression and diminished TAA-directed adaptive immune responses in experimental cancer models.[38-41] Constitutive activation of MEK/ERK signaling has been shown to increase expression of *Csf1* or *Csf2* in certain cancer cells, which could explain increased occurrence of *in situ* proliferated tissue-resident alveolar macrophages in the lungs of *Raf-BxB* mice on a molecular level.[27,42]

Surprisingly, influenza A virus infection caused rapid conversion of the immunosuppressed population of alveolar macrophages in tumor-bearing lungs to an immunologically competent phenotype, as determined by elevated numbers of MHCII- and iNOS-expressing cells and reduced numbers of alveolar macrophages expressing the anti-inflammatory IL-4Rα. We showed by *in vivo* labeling of immune cells that this was indeed due to a functional switch of initially suppressed lung resident macrophages and not to an immigration of macrophages from other lymphoid organs. Concomitantly, impaired phagocytic activity of alveolar macrophages in the lungs of *Raf-BxB* mice was recovered upon IAV infection and was found to be even higher than in alveolar macrophages of WT mice. These results are in full accordance with the previous findings of *Campbell* and colleagues (2015), which described a transition of anti-inflammatory M2-like bone-marrow derived macrophages to a pro-inflammatory (iNOS$^+$, TNFα$^+$) phenotype upon IAV infection *in vitro*.[43] The increased phagocytic activity of alveolar macrophages in the lungs of Raf-BxB mice upon IAV infection does not only reflect the anti-viral properties, but also the anti-tumoral activity, as phagocytosis is one of the major cytotoxic mechanisms of macrophages against cancer cells.[44-46]

Our data furthermore support the hypothesis that repolarization of tumor-associated alveolar macrophages upon IAV infection has a protective role against viral replication. Impaired viral replication in the lungs of tumor-bearing mice was recovered upon clodronate-mediated depletion of alveolar macrophages ([Fig. 6C](#)). The increased number of alveolar macrophages in lungs of tumor-bearing mice and their potential to rapidly switch to a pro-inflammatory phenotype upon IAV infection is responsible for impaired viral replication, reduced lung tissue damage and enhanced survival of *Raf-BxB* mice. Interestingly, our previous study demonstrated increased mortality of transgenic *Raf-BxB* mice compared to WT mice infected with the same dose of a highly pathogenic avian IAV instead of a low pathogenic strain as used here.[22] In this experimental setting viral replication was not affected compared to WT mice and no differences in global immune responses were described. Besides the substantial difference of homozygosity and heterozygosity of the transgenic murine *Raf-BxB* model applied, the discrepancy of the previous study in comparison to our results might be explained by the fundamentally different inflammatory properties of avian- and human-pathogenic influenza viruses. Highly pathogenic avian IAV (HPAIV) suppress pro-inflammatory immune responses in infected macrophages as an immune evasion mechanism.[47] On the contrary, HPAIV infection induces massive lung tissue damage by

uncontrolled expression of inflammatory cytokines (*cytokine storm*) in endothelial cells.[48,49] Low-pathogenic human IAV such as the H1N1 PR8 strain used in this study, share neither these immunosuppressive properties upon macrophage infection, nor does infection with these viruses induce a cytokine storm in infected lungs.[47] Thus, these viruses show completely different lung pathology and immune responses upon infection, explaining the different outcome of viral replication and survival of infected *Raf-BxB* mice in both studies.

The role of macrophage polarization in tumor development has been controversially discussed within the last decades. It is generally accepted that a broad heterogeneity of different macrophage subsets found in tumor environments support tumor growth.[50] The phenotypic polarization of these innate immune cells is highly reversible in response to different stimuli. Thus, several novel medical approaches aim to target the immunosuppressive macrophages or repolarize and convert these cells to pro-inflammatory macrophages to fight tumor cells.[51-53] However, the outcome of such clinical trials remained insufficient, mainly because of the highly immunosuppressive tumor microenvironment and immune evasion mechanisms of tumor cells. Our results demonstrate that influenza A virus infection acts in a dual mode to promote tumor cell lysis. On the one hand, infection leads to direct destruction of tumor cells in an immunocompetent model of NSCLC due to a preferential lytic influenza virus infection. This is in line with results from others obtained *in vitro* and in immunosuppressed *xenograft* models.[26,33] On the other hand, viral infection results in a functional switch of tumor-associated alveolar macrophages from a highly suppressed to a pro-inflammatory state, supporting viral-induced oncolysis of cancer cells. Hence, influenza A viruses possess both a strong lytic as well as an immunostimulatory potential to target non-small cell lung cancer cells *in vivo*. While we used replication competent IAV as a model in our studies, a future medical approach will likely employ controlled infection with attenuated IAV to target NSCLC, especially for treatment of subtypes found to accumulate immunosuppressive macrophages within the tumor microenvironment.

Materials and methods

Animal studies

All experiments were performed with 4-month-old wild type and homozygous transgenic *c-Raf-1-BxB* (*Raf-BxB*) C57Bl/6 mice of both genders that were kept under pathogen-free conditions. The transgenic *Raf-BxB* mice spontaneously develop NSCLC tumors due to expression of the oncogenic Raf kinase under the control of the human surfactant protein C (SP-C) promoter and have been described previously.[34] All animal studies were performed in accordance with the German regulations of the Society for Laboratory Animal Science (GVSOLAS) and the European Health Law of the Federation of Laboratory Animal Science Associations (FELASA). The protocols were approved by the Landesamt für Natur, Umwelt und Verbraucherschutz Nordrhein-Westfalen (LANUV-NRW), Germany.

Mice were anesthetized by inhalation of 2.5% isoflurane (Baxter). For IAV infection, 50 μl of viral stock solution in PBS was intranasally administered. All infection experiments were performed with influenza virus strain A/Puerto Rico/8/34 (PR8, H1N1). The health status of infected animals and body weight loss was monitored daily. The number of infectious virus particles in the BALF was determined by standard plaque assay as previously described[54] and viral titers were expressed as plaque-forming units (pfu) per ml.

For immune cell tracking experiments, 24h before infection mice were anesthetized and 8mM fluorescent CMTMR dye Cell Tracker Orange (CTO, Thermo Fisher Scientific, Cat. No.: C2927) was applied intranasally in a volume of 75 μl per mouse.

RNA isolation, reverse transcription and qRT-PCR

Mouse lungs were collected at indicated time points and total lung RNA was isolated using TRIzol Reagent (Thermo Fisher Scientific, Cat. No.: 15596026). Samples were homogenized (FastPrep-24 homogenizer, MP Biomedicals) and the RNA was precipitated with isopropanol. The precipitated RNA was further purified in a secondary phase separation step as previously described.[55] Purified RNA was transcribed into cDNA using the high-capacity cDNA reverse transcription kit (Thermo Fisher Scientific, Cat. No.: 4368814). Messenger RNA (mRNA) expression levels were determined by TaqMan qRT-PCR using the LightCycler 480 II (Roche Diagnostics). Each cDNA sample was analyzed in triplicate and specific signals were scored in relation to the signal of the housekeeping gene transcript Cytochrome C (CytC). Sequences of primers used for qRT-PCR are listed in Supplementary Table 1.

Immunohistochemistry

Half of the lungs of each mouse was isolated and fixed in 4% paraformaldehyde for 5–7 h at RT, dehydrated in ascending isopropanol dilutions and embedded in paraffin. Paraffin sections of 4 μm were analyzed. Lung specimens were rehydrated and heat-mediated antigen retrieval was performed (10mM citric acid buffer pH 6.0, 20 min). Afterwards paraffin sections were blocked with 10% fetal bovine serum containing 0.1 % Triton-X-100 for 30 min. Antigen-specific staining of human c-Raf-1 and influenza virus NP were performed by incubation with appropriate primary antibodies (rabbit anti-human c-Raf [SP-63], 1:500; goat anti-influenza NP [G105] 1:2500, kind gift of Dr. Robert Webster, Department of Infectious Diseases, St. Jude Children's Research Hospital, Memphis, TN) for 1h at RT followed by species-specific secondary antibody incubation for 30 min. The Vectastain ABC-AP Kit (Vector Laboratories, Cat. No.: AK-5000) was used for visualization of the stained proteins as described in the manufacturer's protocol. Three different sections per mouse lung (approx. 250 μm apart from each other) were quantified from at least 5 mice per each time point. The area of the Raf-positive tumor foci was then measured and expressed in relation to the total section area of the specimen. All analyses were quantified in a blinded manner via the Keyence BZ Analyzer (Keyence).

Analysis of lung immune cell status

Bronchoalveolar lavage (BAL) was performed as previously described.[56] Briefly, mice were euthanized, the trachea was

exposed and the lungs were washed five times with 700 μl PBS containing 2mM EDTA for each wash. Supernatants of the first lavage were kept separately for plaque titration or LDH assay. Cell pellets of the first lavage was combined with cells of the following lavages and centrifuged at 400 g for 10 min at 4°C. Lung tissue from the same mice was minced and digested for 30 min at 37°C in 185.5 U/ml Collagenase (Worthington, Cat. No.: LS004196) and 0.5 mg/ml DNAse I (Roche, Cat. No.: 10104159001) in RPMI. Afterwards lung tissue was filtered through a 70 μm and 45 μm cell strainer and cells were centrifuged at 400 g for 10 min at 4°C. Erythrocytes of BALF- or tissue-derived cells were lysed, cell numbers were determined and the cells were subsequently stained for flow cytometry analysis (Gallios, Beckmann Coulter). Prior to specific staining all samples were incubated with anti-Fcγ RII/III (BD Pharmingen, Cat. No.:5531411) to block non-specific binding of antibodies. Following surface marker staining, intracellular proteins were stained using the BD Cytofix/Cytoperm™ Fixation/ Permeabilization Solution Kit according to manufacturer's protocol (BD Pharmingen, Cat. No.: 554714). Total numbers of immune cells were determined by gating on single cells and normalization to the absolute number of cells counted in the BALF of each individual mouse. Analysis of distinct immune cell populations was performed using the antibodies listed in Supplementary Table 2.

Phagocytosis assay

Bronchoalveolar immune cells were isolated from lungs of mice via BAL as described above. After erythrocyte lysis, cells were counted and equal numbers of immune cells were incubated for 2h with pHrodo™ Red *E.coli* BioParticles™ conjugates for phagocytosis as described by the manufacturer (Thermo Fisher Scientific, Cat. No.: P35361). Prior to specific receptor staining all samples were treated with anti-Fcγ RII/III (BD Pharmingen, Cat. No.: 553141) and were afterwards stained for specific surface markers (CD11c$^+$/F4/80$^+$, see Supplementray Table 2) and were analyzed via flow cytometry (FACSCalibur, BD Biosciences), with respect to pHrodo™ Red *E.coli* BioParticles™ fluorescence as a marker for phagocytic activity.

LDH assay

Lactate dehydrogenase (LDH) assay was performed using an *in vitro* toxicology assay kit (Merck, Cat. No.: TOX7-1KT) according to the manufacturer's protocol. The amount of LDH in the BALF of infected mice was used as a marker of lung tissue damage.

Generation of bone-marrow derived macrophages

Bone marrow-derived cells were isolated from C57Bl/6 mice and after erythrocyte lysis, cells were cultivated for 5 days in RPMI supplemented with 5% fetal bovine serum (FBS), 1% L-gluatmine, 1% non-essential aminoacids, 0,5 mM β-mercaptoethanol, 1mM Na-pyruvate, 50 μg/ml gentamycin and 20% of supernatant of L929 fibroblasts containing M-CSF. After 5 days of cultivation in Petri dishes, macrophages were detached with 10 mM EDTA in PBS and defined numbers were seeded into 96-well plates, either in RPMI with the above mentioned supplements, or with 1:20 diluted BALF. Only first lavages obtained from control uninfected C57Bl/6 and *Raf-BxB* tumor-bearing mice were used. After cultivation of macrophages for 48h, their phenotype was analyzed by flow cytometry as described for immune cells.

Cytotoxicity assay

HeLa cells were incubated for 30 min with 10 μg/ml Mitomycin in suspension to block cell proliferation and seeded with 1×10^4 cells in 100 μl DMEM per well. The next day, bone marrow-derived macrophages that have been pre-stimulated o/n with 1 μg/ml LPS were resuspended in either WT or *Raf-BxB* BALF and added to HeLa cells with 100 μl per well. The final effector-target-cell ration was 20:1 and the final dilution of BALF, 1:20. After 48 h of co-culture, cells were detached and stained for bone-marrow derived macrophage marker. The absolute number of cells per sample was calculated using flow cytometry cell counting beads (Thermo Fisher Scientific, Cat. No.: C36950) as described by the manufacturer and the number of remaining non-lysed HeLa cells was calculated after gating out the CD11b$^+$ and F4/80$^+$ macrophages.

Statistical analysis

Data is expressed as mean $\pm$ SEM. Statistical analysis was performed using GraphPad Prism software (version 6) and the following two-tailed tests: the Mann-Whitney U test when two groups were compared; Kruskal-Wallis test followed by Dunn's comparison analysis when more than two groups were compared; 2-way ANOVA, followed by Sidak's or Dunn's multiple comparisons test when more than one parameter changed in the groups. Results were considered statistically significant at P < 0.05 and displayed as *P < 0.05, **P < 0.01, ***P < 0.001. Mice were allocated randomly into experimental groups after matching for age and gender. Specific numbers of animals can be found in corresponding figure legends.

Disclosure of potential conflicts of interest

The authors report no conflict of interest.

ORCID

Stephan Ludwig 🄳 http://orcid.org/0000-0003-4490-3052

References

1. American Cancer Society. Cancer Facts & Figures 2015. Cancer Facts Fig 2015;2015:1–9.
2. Siegel R, Miller K, Jemal A. Cancer statistics, 2015. CA Cancer J Clin. 2015;65:29.
3. Gabrilovich DI, Ostrand-Rosenberg S, Bronte V. Coordinated regulation of myeloid cells by tumours. Nat Rev Immunol. 2012;12:253–68. doi:10.1038/nri3175.
4. Vetsika EK, Koinis F, Gioulbasani M, Aggouraki D, Koutoulaki A, Skalidaki E, Mavroudis D, Georgoulias V, Kotsakis A. A circulating subpopulation of monocytic myeloid-derived suppressor cells as an independent prognostic/predictive factor in untreated non-small lung cancer patients. J Immunol Res. 2014:659294.
5. Gazdar AF, Linnoila RI, Kurita Y, Oie HK, Mulshine JL, Clark JC, Whitsett J a. Peripheral airway cell differentiation in human lung cancer cell lines. Cancer Res. 1990;50:5481–7.
6. Singh G, Katyal S, Torikata C. Carcinoma of Type II pneumocytes: immunodiagnosis of a subtype of bronchioalveolar carcinomas. Am Assoc Pathol. 1981;102:195–208.
7. Li AR, Chitale D, Riely GJ, Pao W, Miller VA, Zakowski MF, Rusch V, Kris MG, Ladanyi M, Samples T. EGFR Mutations in lung adenocarcinomas clinical testing experience and relationship to EGFR gene. J Mol Diagnostics 2008;10:242–8. doi:10.2353/jmoldx.2008.070178.
8. Gazdar A. Activating and resistance mutations of EGFR in non-small-cell lung cancer: role in clinical response to EGFR tyrosine kinase inhibitors. Oncogene 2009;28:1–14. doi:10.1038/onc.2009.198.
9. Cooper WA, Lam DCL, O'Toole SA, Minna JD. Molecular biology of lung cancer. J Thorac Dis. 2013;5:479–90.
10. Malumbres M, Barbacid M. RAS oncogenes: the first 30 years. Nat Rev Cancer 2003;3:459–65. doi:10.1038/nrc1097.
11. Riva C, Lavieille JP, Reyt E, Brambilla E, Lunardi J, Brambilla C. Differential c-myc, c-jun, c-raf and p53 expression in squamous cell carcinoma of the head and neck: implication in drug and radioresistance. Eur J Cancer Part B Oral Oncol. 1995;31:384–91. doi:10.1016/0964-1955(95)00045-3.
12. Cekanova M, Majidy M, Masi T, Al-Wadei HAN, Schuller HM. Overexpressed Raf-1 and phosphorylated cyclic adenosine $3'-5'$-monophosphatate response element-binding protein are early markers for lung adenocarcinoma. Cancer 2007;109:1164–73. doi:10.1002/cncr.22520.
13. Qiu Z, Wang L, Han J, Liu D, Huang W, Altaf K, Qiu X, Javed MA, Zheng J, Chen B, et al. Prognostic impact of Raf-1 and p-Raf-1 expressions for poor survival rate in non-small cell lung cancer. Cancer Sci. 2012;103:1774–9. doi:10.1111/j.1349-7006.2012.02375.x.
14. Vicent S, López-Picazo JM, Toledo G, Lozano MD, Torre W, Garcia-Corchón C, Quero C, Soria J-C, Martín-Algarra S, Manzano RG, et al. ERK1/2 is activated in non-small-cell lung cancer and associated with advanced tumours. Br J Cancer 2004;90:1047–52. doi:10.1038/sj.bjc.6601644.
15. Masemann D, Boergeling Y, Ludwig S. Employing RNA viruses to fight cancer: novel insights into oncolytic virotherapy. Biol Chem. 2017;398:891–909. doi:10.1515/hsz-2017-0103.
16. Russell S, Peng K-W, Bell JC. Oncolytic virotherapy. Nat Biotechnol. 2014;30:1–29.
17. Pol J, Bloy N, Obrist F, Eggermont A, Galon J, Cremer I, Erbs P, Limacher J-M, Preville X, Zitvogel L, et al. Trial watch: oncolytic viruses for cancer therapy. Oncoimmunology 2014;3:e28694. doi:10.4161/onci.28694.
18. Tong A, Senzer N, Cerullo V, Templeton N, Hemminki A, Nemunaitis J. Oncolytic viruses for induction of anti-tumor immunity. Curr Pharm Biotechnol. 2012;13:1750–60. doi:10.2174/138920112800958913.
19. Weinheimer VK, Becher A, Tönnies M, Holland G, Knepper J, Bauer TT, Schneider P, Neudecker J, Rückert JC, Szymanski K, et al. Influenza a viruses target type II pneumocytes in the human lung. J Infect Dis. 2012;206:1685–94. doi:10.1093/infdis/jis455.
20. Wurzer WJ, Planz O, Ehrhardt C, Giner M, Silberzahn T, Pleschka S, Ludwig S. Caspase 3 activation is essential for efficient influenza virus propagation. EMBO J. 2003;22:2717–28. doi:10.1093/emboj/cdg279.
21. Pleschka S, Wolff T, Ehrhardt C, Hobom G, Planz O, Rapp UR, Ludwig S. Influenza virus propagation is impaired by inhibition of the Raf/MEK/ERK signalling cascade. Nat Cell Biol. 2001;3:301–5. doi:10.1038/35060098.
22. Ölschläger V, Pleschka S, Fischer T, Rziha H-J, Wurzer W, Stitz L, Rapp UR, Ludwig S, Planz O. Lung-specific expression of active Raf kinase results in increased mortality of influenza a virus-infected mice. Oncogene 2004;23:6639–46. doi:10.1038/sj.onc.1207883.
23. Bergmann M, Romirer I, Sachet M, Fleischhacker R, Garcı A, Palese P, Wolff K, Pehamberger H, Jakesz R, Muster T. A genetically engineered influenza a virus with ras -dependent oncolytic properties. Cancer Res. 2001;61:8188–93.
24. García-Sastre A, Egorov A, Matassov D, Brandt S, Levy DE, Durbin JE, Palese P, Muster T. Influenza a virus lacking the NS1 gene replicates in interferon-deficient systems. Virology 1998;252:324–30. doi:10.1006/viro.1998.9508.
25. Muster T, Rajtarova J, Sachet M, Unger H, Fleischhacker R, Romirer I, Grassauer A, Url A, García-Sastre A, Wolff K, et al. Interferon resistance promotes oncolysis by influenza virus NS1-deletion mutants. Int J Cancer 2004;110:15–21. doi:10.1002/ijc.20078.
26. Van Rikxoort M, Michaelis M, Wolschek M, Muster T, Egorov A, Seipelt J, Doerr HW, Cinatl J. Oncolytic effects of a novel influenza a virus expressing interleukin-15 from the NS reading frame. PLoS One 2012;7:e36506. doi:10.1371/journal.pone.0036506.
27. Uemura Y, Kobayashi M, Nakata H, Kubota T, Bandobashi K, Saito T, Taguchi H. Effects of GM-CSF and M-CSF on tumor progression of lung cancer: roles of MEK1/ERK and AKT/PKB pathways. Int J Mol Med. 2006;18:365–73.
28. Ghoneim HE, Thomas PG, Mccullers JA. Depletion of alveolar macrophages during influenza infection facilitates bacterial superinfections. J Immunol. 2013;191:1250–9. doi:10.4049/jimmunol.1300014.
29. Kim HM, Lee Y-W, Lee K-J, Kim HS, Cho SW, van Rooijen N, Guan Y, Seo SH. Alveolar macrophages are indispensable for controlling influenza viruses in lungs of pigs. J Virol. 2008;82:4265–74. doi:10.1128/JVI.02602-07.
30. Takizawa T, Matsukawa S, Higuchi Y, Nakamura S, Nakanishi Y, Fukunda R. Induction of programmed cell death (apoptosis) by influenza virus infection in tissue culture cells. J Gen Virol. 1993;74:2347–55. doi:10.1099/0022-1317-74-11-2347.
31. Hinshaw VS, Olsen CW, Dybdahl-sissoko N, Evans D. Apoptosis : a mechanism of cell killing by influenza A and B viruses. J Virol. 1994;68:3667–73.
32. Mori I, Komatsu T, Takeuchi K, Nakakuki K, Sudo M, Kimura Y. In vivo induction of apoptosis by influenza virus. J Gen Virol. 1995;76:2869–73. doi:10.1099/0022-1317-76-11-2869.
33. Kasloff SB, Pizzuto MS, Silic-Benussi M, Pavone S, Ciminale V, Capua I. Oncolytic activity of avian influenza virus in human pancreatic ductal adenocarcinoma cell lines. J Virol. 2014;88:9321–34. doi:10.1128/JVI.00929-14.
34. Kerkhoff E, Fedorov LM, Siefken R, Walter AO, Papadopoulos T, Rapp UR. Lung-targeted expression of the c-Raf-1 kinase in transgenic mice exposes a novel oncogenic character of the wild-type protein. Cell Growth Differ. 2000;11:185–90.
35. Sobol PT, Boudreau JE, Stephenson K, Wan Y, Lichty BD, Mossman KL. Adaptive antiviral immunity is a determinant of the therapeutic success of oncolytic virotherapy. Mol Ther [Internet] 2009;19:335–44. Available from. doi:10.1038/mt.2010.264.
36. Van Overmeire E, Stijlemans B, Heymann F, Keirsse J, Morias Y, Elkrim Y, Brys L, Abels C, Lahmar Q, Ergen C, et al. M-CSF and GM-CSF receptor signaling differentially regulate monocyte maturation and macrophage polarization in the tumor microenvironment. Cancer Res. 2015;76:35–43. doi:10.1158/0008-5472.CAN-15-0869.
37. Dolcetti L, Peranzoni E, Ugel S, Marigo I, Gomez AF, Mesa C, Geilich M, Winkels G, Traggiai E, Casati A, et al. Hierarchy of

immunosuppressive strength among myeloid-derived suppressor cell subsets is determined by GM-CSF. Eur J Immunol. 2010;40:22–35. doi:10.1002/eji.200939903.

38. Su S, Liu Q, Chen J, Chen J, Chen F, He C, Huang D, Wu W, Lin L, Huang W, et al. A positive feedback loop between mesenchymal-like cancer cells and macrophages is essential to breast cancer metastasis. Cancer Cell 2014;25:605–20. doi:10.1016/j.ccr.2014.03.021.

39. Bronte V, Chappell DB, Apolloni E, Cabrelle A, Wang M, Hwu P, Restifo NP. Unopposed production of granulocyte-macrophage colony-stimulating factor by tumors inhibits CD8+ T cell responses by dysregulating antigen-presenting cell maturation. J Immunol. 1999;162:5728–37.

40. Bayne LJ, Beatty GL, Jhala N, Clark CE, Rhim AD, Stanger BZ, Vonderheide RH. Tumor-derived granulocyte-macrophage stimulating factor regulates myeloid inflammation and T cell immunity in pancreatic cancer. Cancer Cell 2012;21:822–35. doi:10.1016/j.ccr.2012.04.025.

41. Pyonteck SM, Akkari L, Schuhmacher AJ, Bowman RL, Sevenich L, Quail DF, Olson OC, Quick ML, Huse JT, Teijeiro V, et al. CSF-1R inhibition alters macrophages polarization and blocks glioma progression. Nat Med. 2013;19:1264–72. doi:10.1038/nm.3337.

42. Pylayeva-gupta Y, Lee KE, Hajdu CH, Miller G, Bar-sagi D. Oncogenic kras-induced GM-CSF production promotes the development of pancreatic neoplasia. Cancer Cell 2012;21:836–47. doi:10.1016/j.ccr.2012.04.024.

43. Campbell GM, Nicol MQ, Dransfield I, Shaw DJ, Nash AA, Dutia BM. Susceptibility of bone marrow-derived macrophages to influenza virus infection is dependent on macrophage phenotype. J Gen Virol. 2015;96:2951–60. doi:10.1099/jgv.0.000240.

44. Jaiswal S, Jamieson CHM, Pang WW, Park CY, Mark P, Majeti R, Traver D, Rooijen NV, Weissman IL. CD47 is up-regulated on circulating hematopoietic stem cells and leukemia cells to avoid phagocytosis. Cell 2009;138:271–85. doi:10.1016/j.cell.2009.05.046.

45. Munn DH, Cheung NK. Phagocytosis of tumor cells by human monocytes cultured in recombinant macrophage colony-stimulating factor. J Exp Med. 1990;172:231–7. doi:10.1084/jem.172.1.231.

46. Weiskopf K, Weissman IL. Macrophages are critical effectors of antibody therapies for cancer. MAbs 2015;7:303–10. doi:10.1080/19420862.2015.1011450.

47. Friesenhagen J, Boergeling Y, Hrincius E, Ludwig S, Roth J, Viemann D. Highly pathogenic avian influenza viruses inhibit effective immune responses of human blood-derived macrophages. J Leukoc Biol. 2012;92:11–20. doi:10.1189/jlb.0911479.

48. Viemann D, Schmolke M, Lueken A, Boergeling Y, Friesenhagen J, Ludwig S, Roth J. H5N1 Virus activates signaling pathways in human endothelial cells resulting in a specific imbalanced inflammatory response. J Immunol. 2011;186:164–73. doi:10.4049/jimmunol.0904170.

49. Teijaro JR, Walsh KB, Cahalan S, Fremgen DM, Roberts E, Scott F, Martinborough E, Peach R, Oldstone MBA, Rosen H. Endothelial cells are central orchestrators of cytokine amplification during influenza virus infection. Cell [Internet] 2011;146:980–91. Available from. doi:10.1016/j.cell.2011.08.015.

50. Movahedi K, Laoui D, Gysemans C, Baeten M, Stangé G, Van Bossche JD, Mack M, Pipeleers D, In't Veld P, De Baetselier P, et al. Different tumor microenvironments contain functionally distinct subsets of macrophages derived from Ly6C(high) monocytes. Cancer Res. 2010;70:5728–39. doi:10.1158/0008-5472.CAN-09-4672.

51. Rolny C, Mazzone M, Tugues S, Laoui D, Johansson I, Coulon C, Squadrito ML, Segura I, Li X, Knevels E, et al. HRG inhibits tumor growth and metastasis by inducing macrophage polarization and vessel normalization through downregulation of PlGF. Cancer Cell 2011;19:31–44. doi:10.1016/j.ccr.2010.11.009.

52. Duluc D, Corvaisier M, Blanchard S, Catala L, Descamps P, Gamelin E, Ponsoda S, Delneste Y, Hebbar M, Jeannin P. Interferon-γ reverses the immunosuppressive and protumoral properties and prevents the generation of human tumor-associated macrophages. Int J Cancer 2009;125:367–73. doi:10.1002/ijc.24401.

53. Coscia M, Quaglino E, Iezzi M, Curcio C, Pantaleoni F, Riganti C, Holen I, Mönkkönen H, Boccadoro M, Forni G, et al. Zoledronic acid repolarizes tumour-associated macrophages and inhibits mammary carcinogenesis by targeting the mevalonate pathway. J Cell Mol Med. 2010;14:2803–15. doi:10.1111/j.1582-4934.2009.00926.x.

54. Seyer R, Hrincius ER, Ritzel D, Abt M, Mellmann A, Marjuki H, Wolff T, Ludwig S, Ehrhardt C. Synergistic adaptive mutations in the hemagglutinin and polymerase acidic protein lead to increased virulence of pandemic 2009 H1N1 influenza a virus in mice. J Infect Dis. 2012;205:262–71. doi:10.1093/infdis/jir716.

55. Börgeling Y, Schmolke M, Viemann D, Nordhoff C, Roth J, Ludwig S. Inhibition of p38 mitogen-activated protein kinase impairs influenza virus-induced primary and secondary host gene responses and protects mice from lethal H5N1 infection. J Biol Chem. 2014;289:13–27. doi:10.1074/jbc.M113.469239.

56. Köther K, Nordhoff C, Masemann D, Varga G, Bream JH, Gaestel M, Wixler V, Ludwig S. MAPKAP kinase 3 suppresses Ifng gene expression and attenuates NK cell cytotoxicity and Th1 CD4 T-cell development upon influenza a virus infection. FASEB J. 2014;28:4235–46. doi:10.1096/fj.14-249599.